Bridging Palaeoseismic and Geodetic Observations for the AD 1700 Cascadia Earthquake with an Earthquake Cycle Model

Weilun Qin[1], Rob Govers[2], Mario D'Acquisto[3], Natasha Barlow[4], Riccardo Riva[1]

[1]Delft University of Technology, Netherlands, [2]Utrecht University, Netherlands, [3]GFZ, Germany, [4]University of Leeds, United Kingdom

contact: W.Qin@tudelft.nl

Introduction

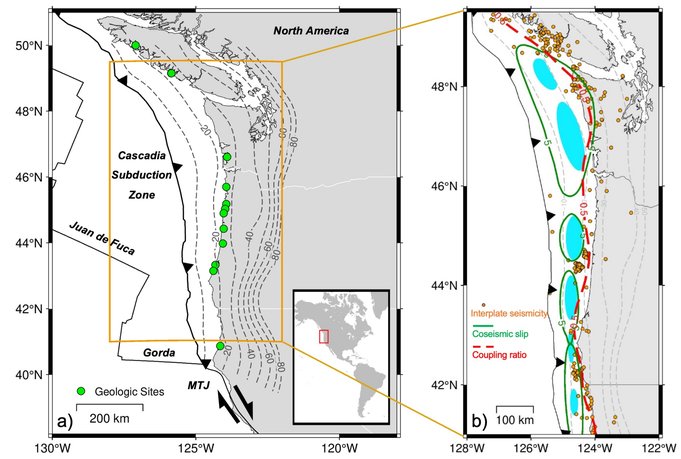

Figure 1. (a) Tectonic settings in the Cascadia subduction zone where the Juan de Fuca plate subducts underneath the North American plate. South of the subduction zone sits the Mendocino Triple Junction (MTJ). Grey contour lines show the depth of the subduction slab. Palaeoseismic sites from Kemp et al. (2018) are shown as green dots. Inset map highlights the Cascadia subduction zone with respect to the Americas. (b) Locked patches (blue) of the earthquake cycle model are compared with interplate seismicity (Morton et al., 2023), modelled coseismic slip (5 m) for the AD 1700 Cascadia earthquake (Wang et al., 2013), and 50% coupling ratio from Li et al (2018).

The study of past earthquakes is important for seismic hazard assessment. Here, we focus on the Cascadia subduction zone where the last great megathrust earthquake occurred in the year AD 1700. We address the following question: **is the current interseismic locking pattern consistent with the last great megathrust rupture along this margin?**

To this end, we develop a 3D quasi-dynamic earthquake cycle model, which includes a realistic slab geometry and simulate the earthquake cycle in a physical consistent manner. The locked patches on the megathrust (blue patches in Figure 1b) accumulate slip deficit interseismically and release it coseismically.

Our model results agree well with both palaeoseismic estimates of coastal subsidence during (and shortly after) the earthquake and GPS estimates of interseismic surface velocities. This suggests that the present-day interseismic locking is consistent with the AD 1700 rupture. We also find that the role of postseismic deformation (in particular afterslip) is not resolved by the palaeoseismic observations.

Subduction Earthquake Model

We build a Cascadia subduction earthquake model based on realistic subducting and overriding plate geometry. This enables us to capture background signals from the complex subduction geometry (Figures 5 and 6). To model the earthquake cycle, we define dynamic boundary conditions on the shallow part (<=80 km) of the slab and place mechanically locked patches on the megathrust. We apply decoupled boundary conditions on the deep part and back side of the slab to exclude the influence from long-term mantle flow.

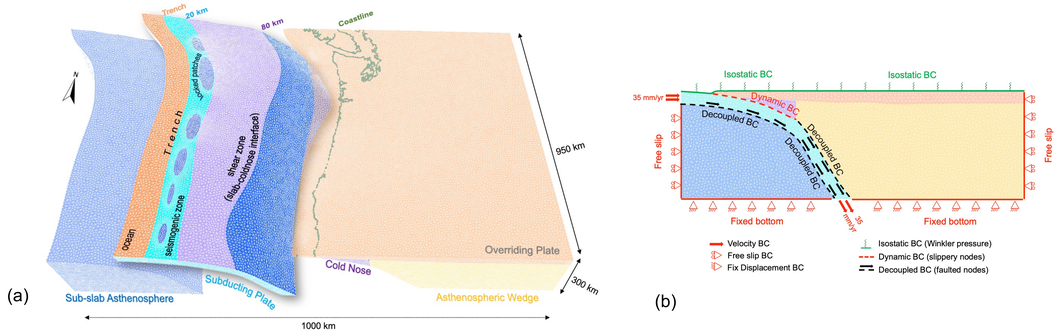

Figure 2. Visualization of the 3D finite-element earthquake cycle model for the Cascadia subduction zone. (a) 3D exploded view on the model components: overriding plate, subducting plate, cold nose, sub-slab asthenosphere, and asthenospheric wedge. Locked patches, seismogenic zone, as well as the shear zone are highlighted on the subducting plate. Both sub-slab asthenosphere and asthenospheric wedge components are viscoelastic with a Maxwell rheology while the other components are elastic. Coastline is highlighted with dark green dots on the overriding plate. (b) 2D cross section view on the plane that parallel to the convergence direction with applied boundary conditions (BCs).

Modelling Earthquake Cycles

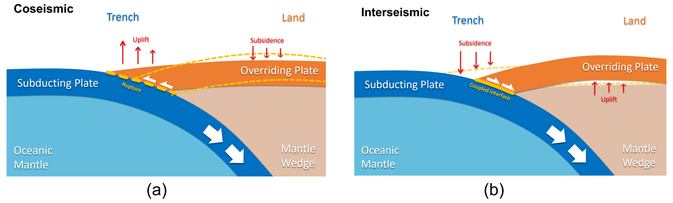

Figure 3. Surface deformation during (a) coseismic and (b) interseismic stages of a subduction earthquake cycle.

We define four different stages during earthquake cycles in our model.

- Coseismic: asperities are unlocked, and the main earthquake occurs
- Afterslip: deeper aseismic slip and aftershocks following the main event
- Postseismic: viscoelastic stress relaxation acts in the upper mantle
- Interseismic: interval between earthquakes after postseismic processes have ended

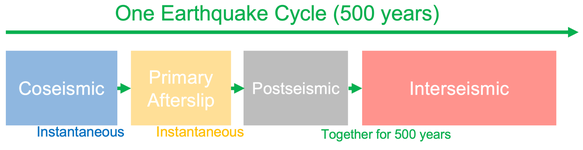

Figure 4. The earthquake cycle set up in our model.

Results for Interseismic Horizontal Velocity and the AD 1700 Coseismic (and Postseismic) Vertical Displacement

- The interseismic results nicely capture the horizontal velocity gradient from the observed subduction-coupled GPS horizontal velocities.
- The interseismic velocity misfits in the southern Cascadia is a result of a uniform convergence rate (35 mm/year) in our model, which is larger than the actual rate in the southern model domain.

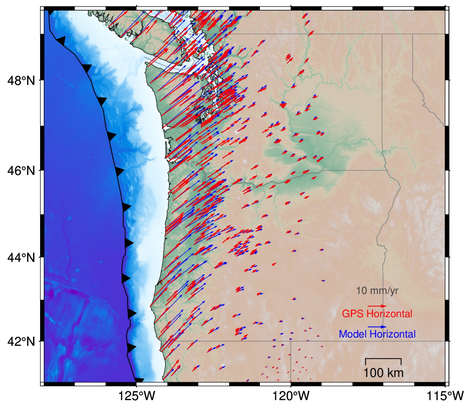

Figure 5. Comparison of modeled interseismic velocities (blue) and subduction-coupled horizontal GPS velocities (red). Modeled velocity field is output 320 years after the earthquake. In this model, continental and sub-slab asthenosphere viscosity is set to 5×10^{19} and 1×10^{20} Pa·s, respectively.

- Releasing asperities coseismically leads to the rebound of the overriding plate, which causes uplift in the offshore overriding plate and subsidence in the onshore part (Figures 3a and 6a). The combined effect of coseismic slip and afterslip leads to less subsidence at the coastal sites (Figures 6b and 6c).
- We show the contribution of different amounts of afterslip (Figure 6c) because the limited resolution of the palaeoseismic record prevents us from constraining its temporal evolution.

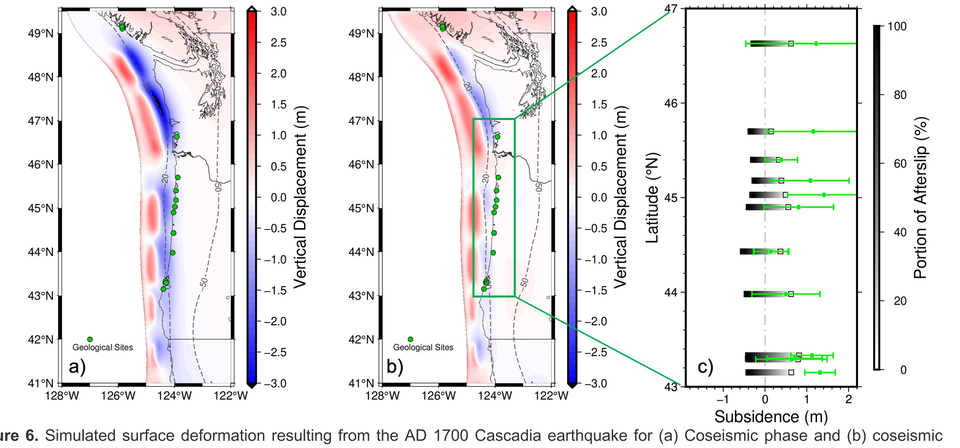

Figure 6. Simulated surface deformation resulting from the AD 1700 Cascadia earthquake for (a) Coseismic phase and (b) coseismic phase with 50% of primary afterslip. (c) Comparison between estimated coastal subsidence (green dots) from Kemp et al. (2018). Error bars illustrate 2-sigma uncertainties. Black squares denote modelled coseismic subsidence, and grey color bars show the portion of afterslip adding to the coseismic results.

This presentation participates in OSPP

Outstanding Student & PhD candidate Presentation contest

References

- **Kemp, A.C. et al. (2018).** Revising Estimates of Spatially Variable Subsidence during the A.D. 1700 Cascadia Earthquake Using a Bayesian Foraminiferal Transfer Function. Bulletin of the Seismological Society of America, 108(2), 654–673.
- **Li, S. et al. (2018).** Geodetically Inferred Locking State of the Cascadia Megathrust Based on a Viscoelastic Earth Model. Journal of Geophysical Research: Solid Earth, 123(9), 8056–8072.
- **McKenzie, K. A., & Furlong, K. P. (2021).** Isolating non-subduction-driven tectonic processes in Cascadia. Geoscience Letters, 8(1), 10.
- **Morton, E.A. et al. (2023).** Cascadia Subduction Zone Fault Heterogeneities From Newly Detected Small Magnitude Earthquakes. Journal of Geophysical Research: Solid Earth, 128(6), e2023JB026607.
- **Wang, P. et al (2013).** Heterogeneous Rupture in the Great Cascadia Earthquake of 1700 Inferred from Coastal Subsidence Estimates. Journal of Geophysical Research: Solid Earth, 118(5), 2460–2473.

Conclusions and Future Steps

- **Conclusions**
  - We reconcile palaeoseismic and geodetic data during and after the AD 1700 Cascadia earthquake by means of a consistent earthquake cycle model
  - The present-day locking pattern is consistent with the AD 1700 earthquake ruptures
  - Primary afterslip reduces the amount of subsidence at the coast, but it is not needed to fit the coseismic estimates from the palaeoseismic record
- **Future Steps**
  - Adding glacial isostatic adjustment (GIA) to the model
  - Separating the signals of both the earthquake cycle and GIA in the palaeo sea-level data

↑ Abstract ↑